Surface, interface, and bulk electronic states of bimetallic superlattices: The case of the Mo/Ta superlattice

Moulay Driss Rahmani and Pierre Masri
Université Montpellier II, Sciences et Techniques du Languedoc, Laboratoire d'Etudes des Surfaces, Interfaces et Composants, Case Courrier 088, place Eugène Bataillon, 34095 Montpellier CEDEX 5, France
(Received 21 October 1991; revised manuscript received 8 April 1992)

This paper presents a theoretical study of the bulk, surface, and interface electronic states of bimetallic superlattices; especially the Mo/Ta superlattice. The calculation of the local density of states at the interface of this particular superlattice allows an examination of the interface phenomena as a function of the coupling parameter at the interface. The superlattice surface study shows that localized surface states may exist in the minigaps.

I. INTRODUCTION

Several studies concerning the structural coherence of metallic superlattices have been published in the past few years. Among these are Nb/Cu,[1,2] Nb/Al,[3] Nb/Ta,[4,5] and Ru/Ir.[6]

These works have proved that the best results are achieved when the two metals that make up the superlattice have the same crystalline structure, and when they have almost identical lattice parameters.

For example, in the case of Nb/Ta superlattices, both components have bcc lattices with the same lattice parameters to within 0.1%. However, a number of published reports describe materials formed by the successive growth of two alternating materials of different crystalline structures [e.g., Ni/Mo (Refs. 7 and 8)]. This is achieved by making use of the influence of different parameters that are relevant to the "matching" of materials made of different chemical species and that belong to different crystalline structures.

Two of the most important achievement are (i) crystallographic parameters: an interesting solution is revealed by considering a bcc crystal (e.g., Nb) grown along one axis [110] top of a fcc substrate crystal (e.g., Cu) grown along another axis [111]; (ii) thermodynamic parameters: the poor miscibility between the atomic species Ru and Ir gives a good epitaxy between their respective structures hcp and fcc.[6]

Superlattice structures may reveal not only electronic properties, but also magnetic features, as shown in a recent investigation of the properties of sandwiches or superlattices made of Ag/Fe or Cr/Fe layers. Additional effects have been measured as (a) a perpendicular magnetization for Ag/Fe sandwiches and superlattices[9–11] and (b) giant magnetoresistance effects for Cr/Fe superlattices.[12]

In this paper, the electronic properties of bimetallic superlattices have been explored by applying the interface response theory to an analytical simple band-structure model within the framework of the tight-binding method. This method has been proven capable of simulating the electronic structure of many systems in solid-state physics. When dealing with surface and interface problems, it is based on a parametrization approach in order to reproduce bulk electronic properties of the system under study. The issued parameters are then useful in discussing physical aspects of the system. This leads to significant qualitative results that retain the main physical features of the system. Numerical calculation-based methods are, nevertheless, sometimes required to reach a better quantitative simulation of the system.

A complete description of how the bimetallic superlattice is built up from the bulk materials will be followed by a presentation of the formalism and a description of the interaction model. The electronic dispersion relations and the local density of states will be derived.

Finally, the theory will be applied to a superlattice consisting of two metallic materials (namely, Mo and Ta), which will provide the example for a discussion of the bulk, surface, and interface electronic properties of such a system. It must be noted that the interface-response theory has already been used in studying certain electronic properties of a polytype semiconductor superlattice.[13,14]

II. FROM THE METAL TO THE SUPERLATTICE—THE FORMALISM

The following is a presentation of the general theory that enables the calculation of the two-layered superlattice response function and, consequently, all electronic properties.

A. The bulk metal

The reference quantity is the bulk-response function $\underline{G}_K$ associated with each material and from which the superlattice is made prior to the superlattice formation. To begin with, the two infinitely extended lattices associated with each material of type K ($K=1,2$) must be taken into account. For each material K, the Hamiltonian $\underline{H}_K$, which contains all required bulk electronic properties,

will be considered. Its elements are expressed by the following:

$$\underline{H}_K = E_K \sum_l C^+(l)C(l) - \gamma_K \sum_{l,\delta} C^+(l+\delta)C(l) , \quad (1)$$

where E_K is the energy of the atomic level for atoms belonging to the metal of type K [see Table I]; $C^+(l)$ and $C(l)$ are, respectively, the creation and the annihilation operators for the atomic site l; and γ_K is the hopping integral for the nearest-neighbor sites. In this expression, l ranges over all sites in the crystal, while δ ranges over the sites selected by the range of the interaction potential within a chosen band-structure model.

The bulk band structure is then simulated using a nearest-neighbors interaction approximation; $\delta_{pp'}=1(0)$ if $p=p'$ (otherwise). The bulk response function $\underline{G}_K$ is then defined by

$$\underline{G}_K(E) = \lim_{\varepsilon \to 0} [(E+i\varepsilon)\underline{I} - \underline{H}_K]^{-1} , \quad (2)$$

where E is the energy, I is the unit matrix, and ε is a small imaginary part. Two mathematical items are then required, namely $\underline{H}_1(\underline{G}_1)$ and $\underline{H}_2(\underline{G}_2)$, in the case of a two-layered superlattice. The bulk electronic spectrum of each separated metal (K) is obtained from the poles of $\underline{G}_K$.

B. The metallic layers

The next step in building up the superlattice is to produce a slab consisting of $L_K(001)$ atomic layers ($1 \le l \le L_K$) from each of these K-type metallic bulk crystals. This is done by switching off all interactions γ_K between the slab-edge layers ($l=1$, and $l=L_K$) and their respective surrounding layers in the embedding metallic medium. The associated Hamiltonian, presumed to correspond to the material of type K located in the nth superlattice cell, is given by the following expression:

$$H(nK;nK) = \sum_{l,l'} V_K(nKl;n'K'l')C^+(l')C(l) , \quad (3)$$

with

$$V_K(nKl;n'K'l') = \gamma_K \delta_{nn'}\delta_{KK'} \times (\delta_{l0}\delta_{l'1} + \delta_{l1}\delta_{l'0} + \delta_{lL_K}\delta_{l',L_K+1} + \delta_{l,L_K+1}\delta_{l'L_K}) . \quad (4)$$

TABLE I. Interaction parameters of molybdenum and tantalum metals. E_0 represents the midband energy, γ is the hopping integral for the nearest-neighbor sites, and Z is the occupation number of the electronic band.

	Molybdenum	Tantalum
E_0 (eV)	0	0.998
γ (eV)	$\frac{1}{2}$	$\frac{7}{12}$
Z	0.5	0.3

In order to adapt the bulk-response functions $\underline{G}_K$ to the different steps in building up the superlattice, a reference function $\underline{G}$ must be introduced. This is defined as a block diagonal matrix formed from the elements of the bulk-response functions $\underline{G}_K$ belonging to the space of definition of each slab

$$G(nKl;n'K'l') = \delta_{mm'}G_m(ll') , \quad (5)$$

where $1 \le l,l' \le L_m = L_K$ and $m=(n,K)$; n is the unit-cell index of the two-layered superlattice; and $\delta_{mm'}$ is the usual Kronecker symbol, defined as $\delta_{mm'}=\delta_{nn'}\delta_{KK'}$ with $\delta_{ij}=1(0)$ if $i=j$ (otherwise).

C. The bulk metallic superlattice

The next step is to couple these different slabs together in order to build up the superlattice. This is achieved by introducing (i) interfacial interactions between two adjacent slabs within the same unit cell n by means of interface hopping integrals $\tilde{\gamma}$ between the nearest-neighbor atomic sites. For example, $\tilde{\gamma}_K$ couples the free surface $l=L_1$ (of slab $K=1$) and $l'=1$ (of slab $K'=2$). This provides a heterostructure, created from the two metallic slabs, which is the elementary kit in building up a two-layered superlattice; (ii) interfacial periodic coupling between an infinite number of such two-layered heterostructures by means of an overlapping integral $\tilde{\gamma}$.

The associated Hamiltonian is expressed by the following:

$$H_I(nK;nK') = \sum_{l,l'} V_I(nKl;n'K'l')C^+(l')C(l) , \quad (6)$$

where

$$V_I(nKl;n'K'l') = -\delta_{nn'}(1-\delta_{K1})(1-\delta_{K2})[\tilde{\gamma}\delta_{lL_K}\delta_{K,K'-1}\delta_{l'1} + \tilde{\gamma}\delta_{l1}\delta_{K,K'-1}\delta_{l',L_K-1}] - \tilde{\gamma}[\delta_{n,n'-1}\delta_{K2}\delta_{K'1}\delta_{lL_2}\delta_{l'1} + \delta_{n,n'+1}\delta_{K1}\delta_{K'2}\delta_{l1}\delta_{l'L_2}] \quad (7)$$

In all the above expressions, the dependence on $\mathbf{k}_\parallel$, the wave vector parallel to the interface planes, and on E, the energy, is not shown for simplicity.

It is now possible to obtain the operator $\underline{A}'_K$ which is defined by the relationship

$$\underline{A}'_K = -\underline{G}_K\underline{V}_K , \quad (8)$$

out of which can be calculated the surface-response operator $\underline{A}'_S$ of the slab K ($l \ge 1, l' \le L_K$).

The elements of $\underline{A}'_S$ are

$$A'_S(Kl;Kl') = -\gamma_K[\delta_{l'1}G_K(l0) + \delta_{l'L_K}G_K(l,L_K+1)] \quad (9)$$

within the nearest-neighbor interaction model.

The corresponding surface-response operator adapted to the superlattice's case is then defined by the equation

$$A'_S(nKl;n'K'l')=\delta_{nn'}\delta_{KK'}A'_S(Kl;Kl') \ . \tag{10}$$

The complete interface response operator A' is given as

$$\underline{A}'=\underline{A}'_S+\underline{V}_I\underline{G} \ . \tag{11}$$

All these steps are necessary in order to calculate the superlattice-response function **g**, which can be done by using the general equation

$$(\underline{I}+\underline{A}')\underline{g}=\underline{G} \ . \tag{12}$$

From this general equation, the following matrix equations are then obtained through standard algebraic calculations:

$$\begin{aligned}\underline{K}(K)&=\begin{bmatrix} g(nKL_K;n'K'l') \\ g(n,K+1,1;n'K'l')\end{bmatrix} \\ &=-\underline{H}(K)\begin{bmatrix} g(n,K-1,L_{K-1};n'K'l') \\ g(nK1;n'K'l')\end{bmatrix} \\ &\quad+\delta_{nn'}\begin{bmatrix} G_K(1l') \\ G_K(L_Kl')\end{bmatrix} ,\end{aligned} \tag{13}$$

where

$$\underline{K}(K)=\begin{bmatrix} A'(nK1;nKL_K) & A'(nK1;n,K+1,1) \\ I(nKL_K;nKL_K)+A'(nKL_K;nKL_K) & A'(nKL_K;n,K+1,1)\end{bmatrix} , \tag{14}$$

$$\underline{H}(K)=\begin{bmatrix} A'(nK1;n,K-1,L_{K-1}) & I(nK1;nK1)+A'(nK1;nK1) \\ A'(nKL_k;n,K-1,L_{K-1}) & A'(nKL_K;nK1)\end{bmatrix} . \tag{15}$$

We also define

$$\underline{P}(K)=-K^{-1}(K)\underline{H}(K) \tag{16}$$

and the transfer matrix between the two equivalent planes of the two-layered superlattice $\underline{R}(m'+2;m')$ as

$$\underline{R}(m'+2;m')=\prod_{m''=m'+1}^{m'+2}\underline{P}(m'') , \tag{17}$$

which complies with the property

$$\det[\underline{R}(m'+2;m')]=1 \quad \text{for all } m' , \tag{18}$$

and where $\prod$ represents the product-operating symbol.

At this point, the bulk dispersion relations for electrons can be easily obtained by solving

$$\mathrm{Tr}[\underline{R}(m'+2;m')]=2\cos(k_zD)=2\eta , \tag{19}$$

where k_z and D are, respectively, the propagation-vector component perpendicular to the layer planes and the superlattice parameter (the distance between two equivalent planes). Tr represents the trace of the argument matrix $\underline{R}$. This dispersion relation is, of course, independent of the values of m' used in (19). To simplify the calculation we have used $m'=0$.

In the particular case where the matrices $\mathbf{g}(nKl;n'K'l')$ are 1×1 matrices (or scalar), the elements are

$$\begin{aligned}g(nKl;n'K'l')=\delta_{nn'}\delta_{KK'}G_K(ll')&-\{[A'(nKl;n,K-1,L_{K-1})A'(nKl;nK1)]\mathbf{P}^{-1}(K) \\ &+[A'(nKl;nKL_K)A'(nKl;n,K+1,1)]\}\begin{bmatrix} g(nKL_K;n'K'l') \\ g(n,K+1,1;n'K'l')\end{bmatrix} \\ &-\delta_{nn'}[A'(nKl;n,K-1,L_{K-1})A'(nKl;nK1)]\underline{H}^{-1}(K)\begin{bmatrix} G_K(1l') \\ G_K(L_Kl')\end{bmatrix} ,\end{aligned} \tag{20}$$

where

$$\begin{bmatrix} g(nKL_K;n'K'l') \\ g(n,K+1,1;n'K'l')\end{bmatrix}=\left[\frac{t}{t^2-1}R(K0)[R(NK')t^{|n-n'|}-R^{-1}(K'0)t^{|n-n'-1|}]+\delta_{nn'}R(KK')\right]K^{-1}(K')\begin{bmatrix} G_{K'}(1l') \\ G_{K'}(L_{K'}l')\end{bmatrix} \tag{21}$$

and

$$t=\begin{cases}\eta-(\eta^2-1)^{1/2}, & \eta>1\\ \eta+i(1-\eta^2)^{1/2}, & -1<\eta<1\\ \eta+(\eta^2-1)^{1/2}, & \eta<-1\end{cases}. \tag{22}$$

Thus, the problem under study here is completely solved in a closed form. The complete interface-response operator can now be calculated and the final electronic energy spectrum of the superlattice can be determined.

This electronic spectrum originates from the modified spectrum of $\underline{G}$. Such modifications arise from the creation of the superlattice as an additional periodicity (band folding) and from the introduction of interactions among the separate material bands that lead to the final band structure.

D. The superlattice surface layer

In order to study the surface electronic structure of the superlattice, a further operator is also required (as with the surface of monocrystals). Using surface-physics terminology, two superlattice free surfaces are created by introducing a "perfect cleavage" plane between the two adjacent slabs, thus, canceling all interactions between these slabs. The associated operator has the following expression:

$$\underline{V}_S(nKl;n'K'l')=\bar{\gamma}[\delta_{n0}\delta_{K2}\delta_{lL_2}\delta_{n'1}\delta_{K'1}\delta_{l'1}+\delta_{n1}\delta_{K1}\delta_{l1}\delta_{n'0}\delta_{K'2}\delta_{l'L_2}]\,. \tag{23a}$$

In the case of the bimetallic superlattice, two surface configurations are possible, depending on whether material 1 or 2 constitutes the top surface layer.

The response function $\underline{g}_s$ associated with the surface of the superlattice is then given by the relationship

$$g_s(nKl;n'K'l')=g(nKl;n'K'l')+\gamma\frac{g(nKl;02L_2)g(111;n'K'l')}{1+\bar{\gamma}g(111;02L_2)}\,. \tag{23b}$$

As far as the surface layer of the superlattice is concerned, one obtains

$$g_s(111;111)=\frac{g(111;111)}{1-\bar{\gamma}g(111;02L_2)}\,. \tag{23c}$$

It can be noted that both response functions $g(111;111)$ and $g(111;02L_2)$ may be calculated by using Eq. (20). The energies of possible superlattice surface electronic states are given by the poles of $g_s(111;111)$.

In our model, no surface states exist for each separate metallic material. In this way, the surface states that may be revealed by the present theory are insured as intrinsic superlattice-induced features.

III. METAL BAND-STRUCTURE MODEL

In this study, a one-band model is used to describe each of the transition metals's d bands. The crystal will be considered to be simple cubic and its d-band electronic structure is described by applying the tight-binding method to a single nondegenerate orbital. As far as the electronic properties of transition metals are concerned, the d electrons play the main role and the d-electron density of states overshadows the s and p densities around the Fermi level. Although the transition metals crystallize in other systems, Allan[15] demonstrated that this model gives good metallic cohesion energy (except for the first period, where the magnetic properties must be incorporated).

The dispersion relation of electrons in the infinitely extended crystal made of material of type K is[16]

$$E_K(k)=E_0-2\gamma_K(\cos k_x a+\cos k_y a+\cos k_z a)\,, \tag{24}$$

where E_0 is the midband energy, γ_K is the overlap integral, a is the lattice parameter, and k_x,k_y,k_z are the wave-vector components. It is already known that $\gamma_K=\frac{5}{12}$ eV for the $3d$ series, $\frac{1}{2}$ eV for the $4d$ series, and $\frac{7}{12}$ eV for the $5d$ series in the periodic table of the elements.

The bulk-associated response function $\underline{G}_K$ is determined by Eq. (2). Let us recall that this function contains all of the required electronic-structure information and it is the reference quantity needed to build up the entire superlattice bulk response function from which the superlattice electronic structure may be obtained.

Assuming that the lattice associated with each material K has an (x,y) in-plane bidimensional periodicity, the $\mathbf{k}_\parallel$ representation can be used to describe the electronic spectrum of $\underline{G}_K$. This representation is aimed at providing a superlattice-adapted expression of $\underline{G}_K$. As the two different metallic slabs (see Sec. II) are incorporated within the superlattice, the interaction model should involve their respective electronic structures. In order to do this, Eq. (2) must first be solved in a closed form between the different (001) atomic planes, labeled by integers l and l'. The ensuing slab-adapted expression is as follows:

$$\underline{G}_K(k_\parallel;l,l';E)=\frac{1}{\gamma_K}\frac{t_K^{|l-l'|+1}}{t_K^2-1}\,, \tag{25}$$

where

$$t_K=\begin{cases}\zeta_K-(\zeta_K^2-1)^{1/2}, & \zeta_K>+1,\\ \zeta_K+i(1-\zeta_K^2)^{1/2}, & -1<\zeta_K<+1,\\ \zeta_K+(\zeta_K^2-1)^{1/2}, & \zeta_K<-1\end{cases} \tag{26}$$

and

$$\zeta_K=\frac{E_K-E}{2\gamma_K}-\cos(k_x a)-\cos(k_y a)\,. \tag{27}$$

Note that the surface-response function associated with a semi-infinite crystal and built up from this latter quantity [Eq. (25)] by canceling interactions between two adjacent planes, has no poles. This means that the simulated semi-infinite crystal has no electronic surface states.

When identifying superlattice electronic surface states, this hypothesis is extremely important. It supports our idea that any surface electronic property revealed by

these calculations is due to an intrinsic superlattice effect rather than to an alteration of a slab-associated surface state.

IV. SUPERLATTICE ELECTRONIC STRUCTURE

In the following, the interface-response-function theory is applied in order to study the electronic properties of bimetallic superlattices. The detailed algebraic calculations are given in Ref. 17.

A. The bulk electronic structure

The electron-dispersion relation is expressed by the following equation:

$$2\eta(\mathbf{k}_{\parallel};E)=2\cos(k_z D) \ . \tag{28}$$

k_z and $k_{\parallel}$ are the wave-vector components perpendicular and parallel to the interface, and $D=\sum_{K=1}^{2} L_K a_K$ is the superlattice period. D has a simple form when the two metals have the same parameter ($a_1=a_2=a$):

$$D=a\sum_{K=1}^{2} L_K \ , \tag{29}$$

where L_K is the number of atomic layers in each metallic slab K.

If the following notations are adopted;

$$t_K=\exp(q_K) \ , \tag{30}$$

$$A_K=\frac{\tilde{\gamma}}{\gamma_K}\frac{\sinh q_K(L_K-1)}{\sinh q_k} \ ,$$

$$B_K=\frac{\gamma_K}{\tilde{\gamma}}\frac{\sinh q_K(L_K+1)}{\sinh q_K} \ , \tag{31}$$

$$C_K=\frac{\sinh q_K L_K}{\sinh q_K} \ ,$$

and Eq. (28), the dispersion relation of the bulk-electronic states of bimetallic superlattices takes the following form:

$$2\eta(k_{\parallel};E)=-2C_1C_2+B_1B_2+A_1A_2 \ . \tag{32}$$

This relation enables the extraction of the electronic energy allowed in the superlattice for a given $\mathbf{k}_{\parallel}$.

B. The surface electronic structure

As already mentioned, there are two surface configurations in the case of a semi-infinite bimetallic superlattice. In order to study electronic surface states, the key quantities derived from the surface response function are

$$D(K;K')=\tilde{\gamma}(C_K A_{K'}-B_K C_{K'}) \tag{33}$$

and

$$A(E;K,K')=A_K A_{K'}-C_K C_{K'} \ . \tag{34}$$

D is the denominator of g_S [Eq. (23c)]. The zeros of D give us the energies of electronic surface states; $t=A^{-1}(E;K,K')$ is the decaying factor of associated wave functions. Such surface states are well localized if t satisfies the following condition:

$$|t(E_s)|=|A^{-1}(E;K,K')|<1 \ . \tag{35}$$

C. The local density of states

The surface metallic response function associated with material K is

$$G_K(k_{\parallel};11;E)=\frac{t_K}{\gamma_K} \ , \tag{36}$$

where t_K is complex if $|\zeta_K|<1$ [see Eq. (26)]. The local density of states (LDOS) for the first surface-metal plane is given by the equation

$$\delta_K=-\frac{1}{\pi\gamma_K}\sum_{k_{\parallel}}(1-\zeta_K^2)^{1/2} \ , \tag{37}$$

where the summation is performed over the bidimensional Brillouin zone. Symmetry requirements may simplify the numerical calculations here.

In the same manner, the interface density of states between two slabs of the superlattice is given by the following expression:

$$\Delta_K=-\frac{1}{\pi}\sum_{k_{\parallel}}\mathrm{Im}g(n,K=1,l=1;n',K'=1,l'=1) \ , \tag{38}$$

where g is the interface-superlattice response function. It is this formula that enables an examination of the interface phenomena. At this point, these results will be applied to the study of the electronic properties of Mo/Ta superlattices.

V. ELECTRONIC STRUCTURE OF A Mo/Ta SUPERLATTICE

Molybdenum and tantalum are both transition metals. Their lattice parameters are, respectively, equal to 3.30 and 3.15 Å, and they crystallize into the same bcc structure. The Mo/Ta superlattices with superlattice wavelengths in the range of 20–180 Å were made by a sputter deposition technique.[18] Such superlattices grow along the crystallographic axis [110]. In this study, a structural coherence was found extending over many layers as deep as 300 Å within both metals. These crystallites are highly textured in the [110] direction, ±7%, but are randomly oriented in the sample plane. The observed interdiffusion extends over 4 Å.

In Table I the interaction parameters calculated with the help of the one-band model are presented. When the two metals are brought into contact, the Fermi levels become aligned. Here, zero has been chosen to be the Fermi energy.

Concerning the choice of the overlapping integral $\tilde{\gamma}$ value, the common procedure is to take the mean of the two bulk values (γ_1 and γ_2) for $\tilde{\gamma}$:

$$\tilde{\gamma}=x\gamma_1+(1-x)\gamma_2, \quad \text{with } 0\le x\le 1 \ , \tag{39}$$

where x is the weight factor. This simulates the concrete situation of the existence of a disrupted interfacial zone.

The choice of the weight factor x will depend on the number of atoms of each material in the interfacial zone. The value of x will first be considered as equal to 0.5, corresponding to an arithmetic average. This hypothesis enables the calculation of the superlattice electronic band structure without taking into account the influence of the interface phenomena. Now, the dispersion relations using two wave-vector representations will be presented.

A. $k_{\parallel}$ representation

In Fig. 1 the variation of the energies of bulk and surface electronic states of the Mo-Ta superlattice is plotted according to S, a reciprocal two-dimensional parameter related to the $k_{\parallel}$ by the relationship

$$S = \cos(k_x a) + \cos(k_y a) \ . \tag{40}$$

This figure corresponds to the two-atomic-plane-thick films ($L_1 = L_2 = 2$) in order to avoid the complexity of the existence of too many bands. We start with a configuration in which the two metals are infinitely separated—this gives the two bands represented in Fig. 1 (dashed-dotted lines for tantalum and dotted lines for molybdenum). The next step is to form the superlattice structure with these two materials. This, in turn, triggers the formation of four subbands separated by minigaps.

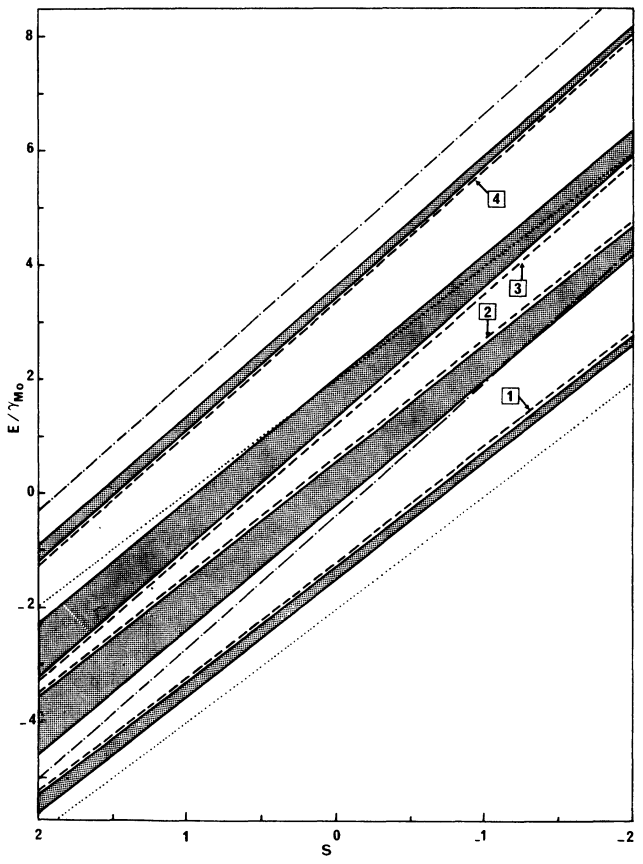

FIG. 1. Bulk and surface electronic states for a Mo/Ta superlattice made of films with $L_1 = L_2 = 2$ atomic planes. The origin of energy is taken at the Fermi energy E_F. The bands are drawn as a function of $S = \cos(k_x a_0) + \cos(k_y a_0)$. The cross-hatched area corresponds to the bulk bands of the superlattice. The surface states are given, respectively, for Mo (1 and 2) at the surface and for Ta (3 and 4) at the surface. The dotted (or the dashed-dotted) lines represent the bulk-band limit of Mo (or Ta).

The $\mathbf{k}_{\parallel}$ representation of the dispersion relations may be used if it is assumed that the periodicity is preserved only in lattice planes parallel to the interface between the two metals, thus implying that the wave-vector component k_z (perpendicular to the interface) is no longer a good quantum number. Consequently, it must be varied between $-\pi/a$ and π/a (its bulk limits) in order to generate the continuum of dispersion relations fitting the above periodicity requirements prevailing in the superlattice. In this way, the upper and lower energies of each subband are generated and an energy-representation frame is obtained, which is then adapted to all electronic structures associated with defects having the same (x,y) in-plane periodicity. This means that resonant states induced by the defect may have their energies falling within one of this continuum's subbands, while the energies of true defect-associated localized states are situated within the minigaps separating these subbands.

It is worthwhile to display the separated-metal bands alongside the superlattice subbands. This is a straightforward way to examine how superlattice electronic features are related to their source bands. For example, it can be better understood why the highest superlattice subband has a marked tantalum nature while the lowest one has a more pronounced molybdenum nature. Strong overlapping between separated-metal bands leads to the formation of the remaining two subbands. The same conclusion was also obtained with another calculation technique in the case of Nb/Ta (001) superlattices.[19]

The aforementioned may explain why the low-energy superlattice surface states (Fig. 1, curves 1 and 2) are obtained when molybdenum constitutes the superlattice's top surface, while high-energy superlattice surface states (Fig. 1, curves 3 and 4) are obtained when the semi-infinite superlattice ends in a tantalum layer. At this point, a change will be made at the interfaces in the interaction parameter $\tilde{\gamma}$ in order to determine its influence on the superlattice's electronic structure.

When the weight factor x is varied between 0 and 1 the subbands remain almost unchanged. This means that as long as the values of $\tilde{\gamma}$ are fixed by a mean rule, such as the one given in Eq. (39), the interface has an insignificant effect on the electronic structure. Superlattice effects dominate in order to fix the relative position and the width of these subbands. However, more pronounced interface effects may be obtained if highly asymmetric values of $\tilde{\gamma}$ (relative to γ_{Mo} and γ_{Ta}, respectively) are chosen.

The results obtained for the Mo/Ta superlattice are shown in Fig. 2. The three values of $\tilde{\gamma}$ are (1) $\tilde{\gamma} = \gamma_{\mathrm{Mo}} - 0.1$ eV corresponding to a weak interface interaction; (2) $\tilde{\gamma} = \gamma_{\mathrm{Ta}} + 0.1$ eV corresponding to a strong interface coupling; and (3) $\tilde{\gamma} = (\gamma_{\mathrm{Mo}} + \gamma_{\mathrm{Ta}})/2$, an arithmetic average. In the first two situations, small subband shifts occur (upwards and downwards). The subband

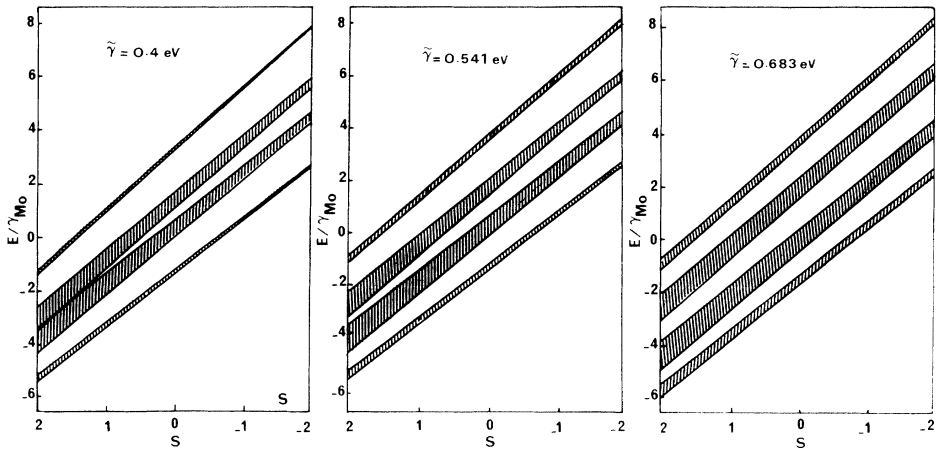

FIG. 2. Bulk electronic bands of a Mo/Ta superlattice with different values of the coupling parameter $\tilde{\gamma}$ (as depicted on the figures).

widths increase as $\tilde{\gamma}$ increases, thus reinforcing the superlattice character of the structure. This results in a more significant dispersion of the subbands. Therefore, the strength of the shifting of the subbands decreases as the metal's slabs become thicker.

B. $(k_z, \mathbf{k}_\parallel = \mathbf{0})$ representation

Figure 3 illustrates the dependence of the superlattice subbands dispersion on the slab thickness. The small squares indicate the electronic-surface-states's positions in association with the metal (molybdenum, full; tantalum, empty) at the superlattice's surface. The numbers near these surface-state levels give the decay factor $t(E_s)$ [Eq. (35)] of the corresponding wave function. Five different thicknesses have been studied here ($L_1 = L_2 = 2$, 3, 4, 5, and 6).

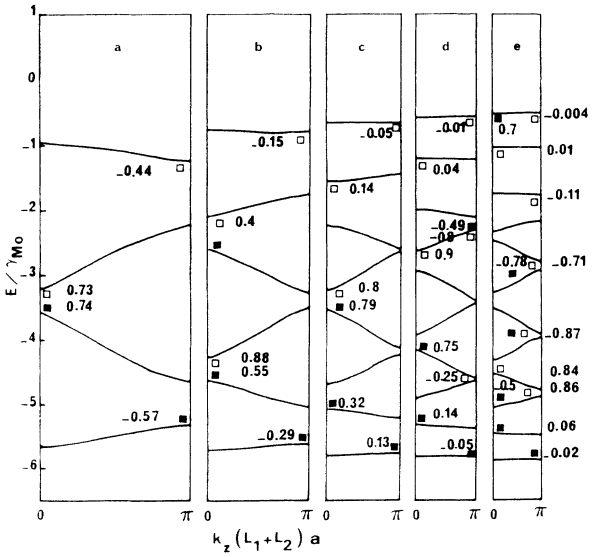

FIG. 3. Dispersion of the bulk bands at the center of the reduced bidimensional Brillouin zone ($\mathbf{k}_\parallel = \mathbf{0}$) in function of k_z for several film widths; $L_1 = L_2 = L$ varies here from 2 to 6: (a) $L = 2$; (b) $L = 3$; (c) $L = 4$; (d) $L = 5$; (e) $L = 6$. $\tilde{\gamma} = 0.542$ eV; the other parameters are given in Table I. ■ corresponds to Mo at the surface and □ to Ta at the surface.

As the thickness of the slabs increases, the Brillouin zone is reduced. This produces a folding of the electronic bands and an opening of gaps in which surface states may exist. Concerning the electronic surface states in the minigaps, it can be noted that less localized states (small $|t(E_s)|$) are close to the large-width subbands, and that very localized states are situated near very flat bulk subbands. In fact, the flat bands are derived from the metal at the superlattice's surface, but the others are the result of the overlapping of the two metals's bulk bands. Consequently, the associated surface states decay slowly inside the bulk. This result is even more pronounced when the slab thicknesses are increased.

The calculation of the local density of states at the metal surface and at the interface for the Mo/Ta superlattice will now be presented. In the case of the Mo/Ta superlattice, this calculation provides complementary information concerning the interface influence on the superlattice's electronic structure. The following is a summary of these calculations.

C. The local density of states

In general, the LDOS of a system is derived from the imaginary part of its response-function trace. In this study, the LDOS at the surface plane of one metal will be calculated, followed by the calculation of the interface LDOS in the case of Mo/Ta superlattice.

1. The metal-surface LDOS

In Eq. (37), the sum over the domain of the two-dimensional Brillouin zone is calculated with the help of the special points method.[20] In Fig. 4, the LDOS computed at the surface plane for molybdenum and tantalum surfaces is plotted. E_F is taken as the origin of the energies and, because the occupation number of the molybdenum $Z = 0.5$, the associated midband energy E_0 coincides with the Fermi level. Both the molybdenum and tantalum curves show a maximum density of states for energies respectively equal to the associated Mo- or Ta-

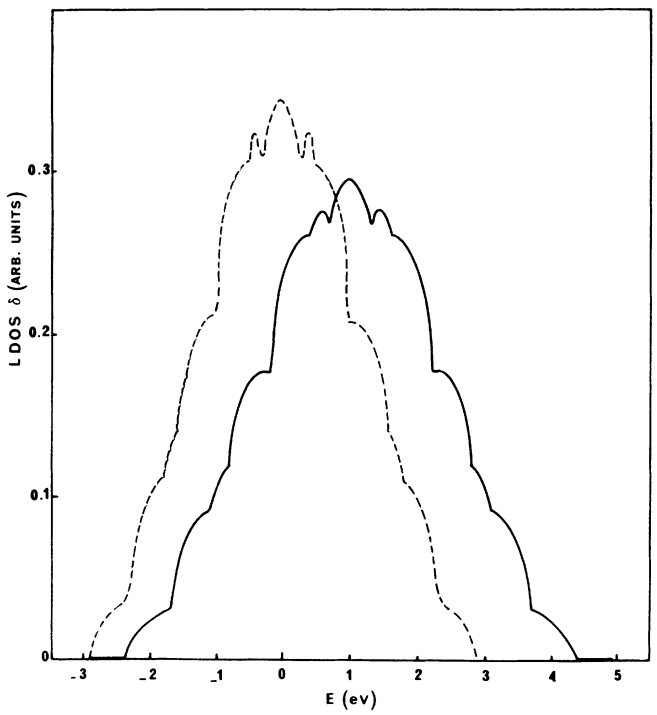

FIG. 4. LDOS at the Mo (— — —) or Ta (——) surface of the corresponding crystal. The origin in energy is taken at the Fermi energy E_F. The scale of the density of states is in arbitrary units. The parameters are given in Table I.

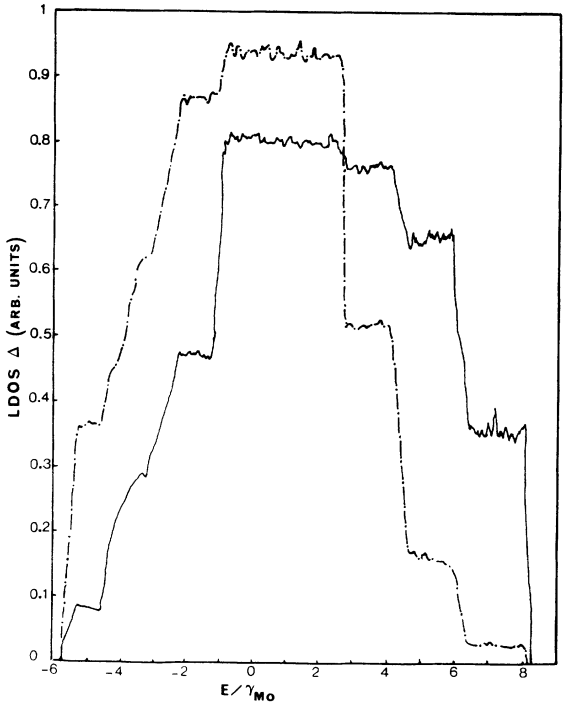

FIG. 5. LDOS at an interfacial atomic layer made of Mo (—·—) or Ta (——) in a Mo/Ta superlattice. The scale of density of states is in arbitrary units. $L=L_1=L_2=2$.

like atomic levels. The d band of molybdenum is half filled, while that of the tantalum contains three electrons, thus resulting in a higher density for molybdenum. The different shape anomalies present on both curves are due to the discrete nature of the summation over the Brillouin zone and, therefore, have no physical meaning.

2. *The interface LDOS of the Mo/Ta superlattice*

At this point, the shape of the interface LDOS and its evolution with the thickness and the interface coupling will be examined. In Fig. 5, the interface LDOS of the Mo/Ta superlattice is plotted as a function of the energy normalized to γ_{Mo}. The dashed line represents the tantalum plane at the interface, while the solid line represents the molybdenum plane. This figure corresponds to two-atomic-plane-thick films ($L_1=L_2=2$).

These plots have been obtained by taking the arithmetic mean of the two bulk values of the interaction parameters across the interface. The plots have the same shape, but the energy shifts are at higher values for the tantalum (lower for the molybdenum) interface plane. This agrees with the previous idea comparing the superlattice subbands's nature with the nature of the metals.

In a previous study,[21] the effect of the interface coupling has been examined by analyzing the LDOS where two sharp peaks, symmetrical with respect to the center of the LDOS, appear. In order to assess their findings, the authors of Ref. 21 considered the limit case of a very strong intermetallic coupling. This presents the advan-

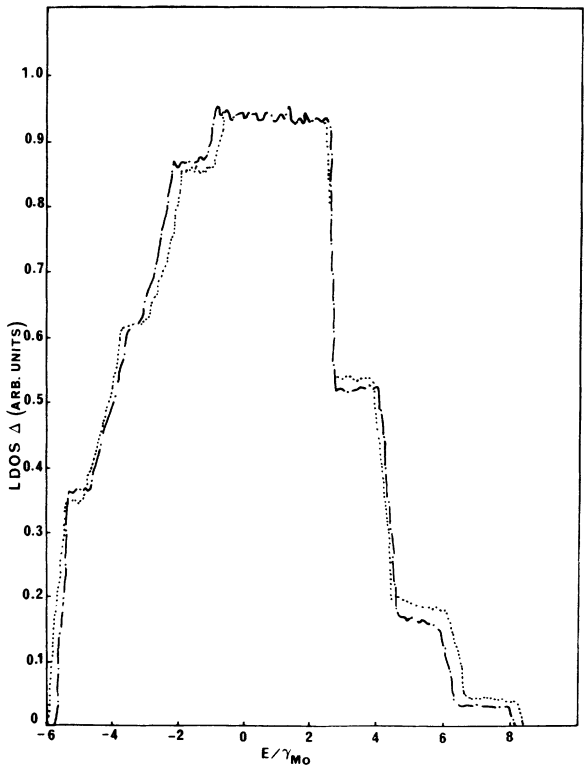

FIG. 6. LDOS at an interfacial Mo atomic plane of a Mo/Ta superlattice for two values of the interslab coupling parameters: $\tilde{\gamma}=0.542$ eV (—·—); $\tilde{\gamma}=0.683$ eV (...); $L=L_1=L_2=2$. The scale of density of states is in arbitrary units.

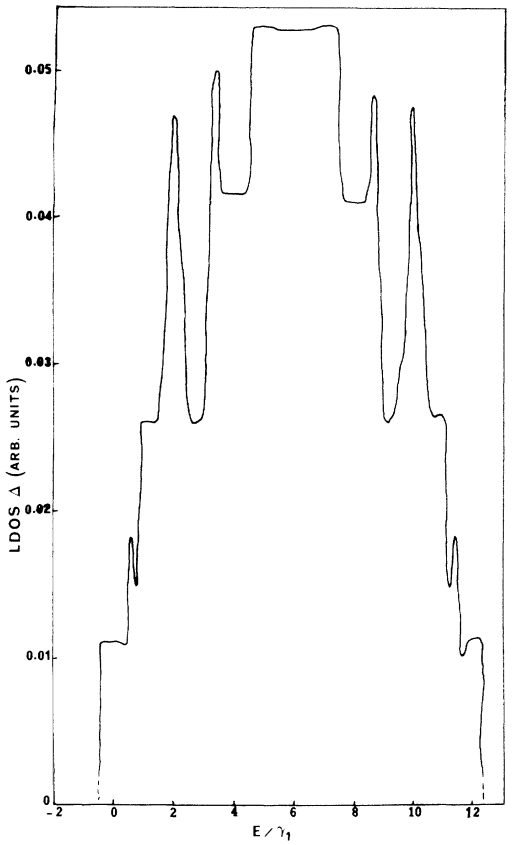

FIG. 7. Interfacial LDOS in a superlattice made of the same metal. This situation may simulate a stacking fault in the superlattice. $\gamma_1=1$ eV; $E_1=6$ eV; $\gamma_2=1$; $E_2=6$; $\tilde{\gamma}=2$; $L_1=L_2=L=5$. The scale of density of states is in arbitrary units.

tage of amplifying the effect rather than considering a real physical situation. It has thus been shown that such states do indeed exist for the case of two semi-infinite metal layers.[22]

In this study, the effect of the interface coupling $\tilde{\gamma}$ is also considered in two different cases. In the first one (Fig. 6), physically reasonable values of $\tilde{\gamma}$ are used. The second (Fig. 7) considers strong values of $\tilde{\gamma}$ in order to enhance the interface states's features.

It can be seen that the results of these two cases agree with those of other calculations.[21] This definitely establishes the local rather than superlattice-interfacial nature of the states. The relatively strong electronic interface coupling $\tilde{\gamma}$ significantly extends the range of allowed states at the interface. These states are confined within the interface layer, but propagate parallel to the interface.[21] They thus have a two-dimensional nature. In general, it seems that interface-state formation would be undesirable from the point of view of improving superconducting properties.

VI. CONCLUSION

In this paper, the electronic properties of bimetallic superlattices have been studied with the help of the interface-response-function theory. The one-band model, which has been used to describe transition-metal electronic properties, has the following approximations: (1) all hopping integrals, except for the nearest-neighbor sites, are assumed to be zero; (2) the magnetic effects in transition metals are neglected; (3) the semi-infinite metals from which the superlattice is constructed have no electronic surface states.

The simplicity of this model enables us to derive, in a closed form, the analytic quantities from which the bulk, surface, and interface phenomena are studied. The application to the Mo/Ta superlattice shows that the periodicity along the growth axis produces a folding of the electronic bands in the associated reduced Brillouin zone, and also, an opening of additional gaps in which surface states may exist. The energy position and the degree of localization of these surface states depend on layer thickness and on the nature of the metallic slab at the superlattice's surface. The dispersion of the electronic subbands depends on the interface coupling.

ACKNOWLEDGMENT

The Laboratoire d'Etudes des Surfaces, Interfaces et Composants is Unité Associée au Centre National de la Recherche Scientifique No. D 07870.

[1]I. K. Schuller, Phys. Rev. Lett. **44**, 1597 (1980).
[2]W. P. Lowe, T. W. Barbee, Jr., T. H. Greballe, and D. B. McWhan, Phys. Rev. B **24**, 6193 (1981).
[3]J. Geerk, M. Gurvitch, D. B. McWhan, and J. M. Rowell, Physica B and C **109&110B**, 1175 (1982).
[4]S. M. Durbin, J. E. Cunningham, M. F. Mochel, and C. P. Flynn, J. Phys. F **11**, L223 (1981).
[5]S. M. Durbin, J. E. Cunningham, and C. P. Flynn, J. Phys. F **12**, L75 (1982).
[6]J. E. Cunnigham and C. P. Flynn, J. Phys. F **15**, L221 (1985).
[7]S. T. Ruggiero, T. W. Barbee, and M. R. Beasley, Phys. Rev. Lett. **45**, 1299 (1980).
[8]M. R. Kahn, C. L. S. Chun, G. P. Felcher, M. Grimsditch, A. Kuery, C. M. Falco, and I. K. Schuller, Phys. Rev. B **27**, 7186 (1983).
[9]B. Heinrich, K. B. Urquhart, A. S. Arrott, J. F. Cochran, K. Myrtle, and S. T. Purcell, Phys. Rev. Lett. **59**, 1756 (1987).
[10]N. C. Koon, B. T. Jonker, F. A. Volkening, J. J. Krebs, and G. A. Prinz, Phys. Rev. Lett. **59**, 2463 (1987).
[11]R. Cabanel, P. Etienne, S. Lequien, G. Creuzet, A. Barthelemy, and A. Fert, J. Appl. Phys. **67**, 5409 (1990).
[12]M. N. Baibich, J. M. Broto, A. Fert, F. Nguyen Van Dau, F. Petroff, P. Etienne, G. Creuzet, A. Friederich, and J. Chazelas, Phys. Rev. Lett. **61**, 2472 (1988).
[13]M. D. Rahmani, P. Masri, and L. Dobrzynski, J. Phys. C **21**, 4761 (1988).
[14]P. Masri and M. D. Rahmani, Phys. Rev. B **40**, 1175 (1989).
[15]G. Allan, Ann. Phys. **5**, 169 (1970).

[16]B. Djafari-Rouhani, L. Dobrzynski, and P. Masri, Phys. Rev. B **31**, 7739 (1985).
[17]P. Masri and L. Dobrzynski, Surf. Sci. **198**, 285 (1988).
[18]C. M. Falco, W. R. Bennett, and A. Boufelfel, in *Dynamical Phenomena at Surfaces, Interfaces and Superlattices,* edited by F. Nizzoli, K. H. Rieder, and R. F. Willis (Springer-Verlag, Berlin 1985), p. 35.
[19]V. R. Velasco, R. Baquero, R. A. Brito-Orta, and F. Garcia-Moliner, J. Phys. Condens. Matter **1**, 6413 (1989).
[20]S. L. Cunnigham, Phys. Rev. B **10**, 4988 (1974).
[21]M. Menon and G. B. Arnold, Phys. Rev. B **27**, 5508 (1983).
[22]A. Yaniv, Phys. Rev. B **17**, 3904 (1978).

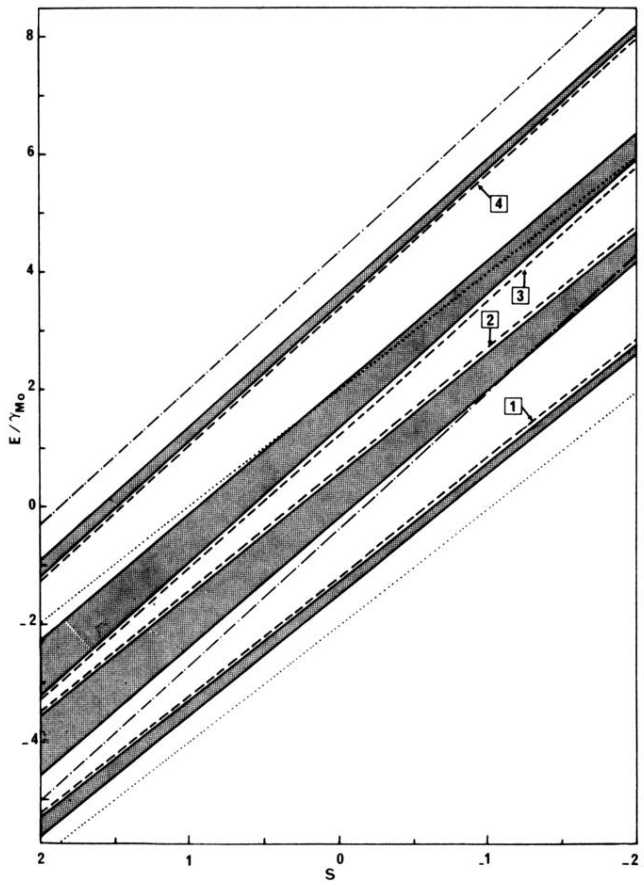

FIG. 1. Bulk and surface electronic states for a Mo/Ta superlattice made of films with $L_1=L_2=2$ atomic planes. The origin of energy is taken at the Fermi energy E_F. The bands are drawn as a function of $S=\cos(k_x a_0)+\cos(k_y a_0)$. The cross-hatched area corresponds to the bulk bands of the superlattice. The surface states are given, respectively, for Mo (1 and 2) at the surface and for Ta (3 and 4) at the surface. The dotted (or the dashed-dotted) lines represent the bulk-band limit of Mo (or Ta).